# Crystal and Molecular Structure of $[Ni(Me_4[14]hexaenatoN_4)]_2(CF_3SO_3)_2$: Conversion of a Metal-Stabilized $\pi$-Radical to a Diamagnetic Dimer with a Long Metal–Metal Bond and Eclipsed Macrocyclic Ligands upon Crystallization

**S.-M. Peng,[1a] James A. Ibers,*[1a] M. Millar, and R. H. Holm[1b]**

*Contribution from the Departments of Chemistry, Northwestern University, Evanston, Illinois 60201, and Massachusetts Institute of Technology, Cambridge, Massachusetts 02139.* *Received May 17, 1976*

**Abstract:** In dilute nonaqueous solutions the tetraaza macrocyclic complex $[Ni(Me_4[14]hexaenatoN_4)]^+$ exists as a monomeric paramagnetic species, whose spectrum has previously been analyzed in terms of a Ni(II)-stabilized 15-$\pi$ electron cation radical with the unpaired electron delocalized over the 14-membered ring system. However, as shown by the present three-dimensional x-ray diffraction study, the cation in the crystalline state forms a diamagnetic dimer. The trifluoromethanesulfonate salt crystallizes with one dipositive dimer per unit cell in the triclinic space group $C_i^1$-$P\bar{1}$ with $a$ = 12.069 (2) Å, $b$ = 11.889 (2) Å, $c$ = 7.157 (1) Å, $\alpha$ = 98.28 (1)°, $\beta$ = 105.25 (1)°, and $\gamma$ = 60.04 (1)° at −117 (3) °C. The structure has been refined anisotropically by full-matrix least-squares techniques to conventional and weighted $R$ indices of 0.049 and 0.084, based on 1978 observations ($I \geq 3\sigma(I)$). There are number of unusual features associated with the structure. First, the dimers contain a weak Ni–Ni bond of length 3.063 (1) Å. Secondly, the macrocylic ligands of the dimers are eclipsed, maximizing rather than minimizing nonbonding interactions. Thirdly, the double bonds of the macrocyclic ligand are essentially delocalized. A qualitative bonding scheme is applied to account for these features.

Among the recent developments in the chemistry of tetraaza macrocyclic metal complexes has been the discovery of facile oxidative dehydrogenation reactions which increase the extent of ligand unsaturation without alteration in ligand framework. For example, the 12-$\pi$ complexes $M(Me_4[14]tetraenatoN_4)$ (**1**, M = Ni(II), Pd(II), Cu(II)) can be smoothly converted to the cation **2** ($[ML]^+$), which in turn can be reduced to the neutral complex **3** and oxidized to the dication **4**.[2,3]

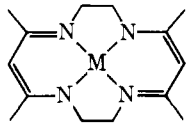

1

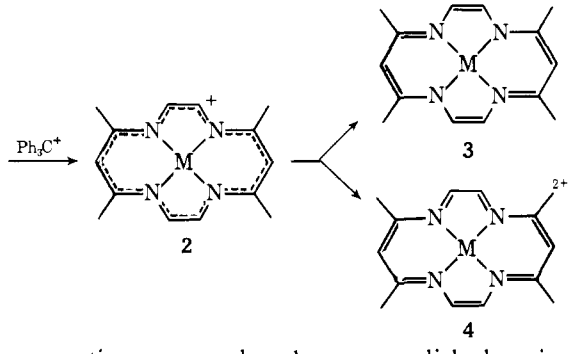


2 3 4

Similar reactions can also be accomplished using $M(Ph_2[14]tetraenatoN_4)$ complexes,[4] and with M = Ni(II) lead to an analogous series of species.[5] The corrinoid ring system is accessible by oxidative dehydrogenation of $M(Ph_2[15]tetraenatoN_4)$ complexes.[5]

Electrochemical measurements have demonstrated the existence of the three-membered electron transfer series **3** ⇌ **2** ⇌ **4**.[2] In dilute (~$10^{-3}$ to $10^{-4}$ M) nonaqueous solutions the intermediate member of the Ni series, $[NiL]^+$, exists predominantly or exclusively as monomeric paramagnetic species. The complex EPR spectrum, consisting of over 80 resolved lines, has been analyzed in considerable detail.[3] From this analysis it has been concluded that the unpaired electron is delocalized over the entire 14-membered ligand ring systems, $\pi$-spin density on the metal is small or zero, and the complex closely approaches the limiting formulation $[Ni^{II}L\cdot^-(15\pi)]^+$ with a probable $^2B_{1u}$ ground state ($D_{2h}$ symmetry). Consequently, the redox events in the electron transfer series can be regarded as restricted to the ligand system, which is of the tetraaza[14]annulene type.

In more concentrated solutions EPR and spectrophotometric observations have indicated the probable existence of the equilibrium $2[NiL]^+ \rightleftharpoons [NiL]_2^{2+}$,[2,3,6] which, however, has proven difficult to quantitate. Crystallization of $BF_4^-$ and $CF_3SO_3^-$ salts from such solutions has yielded diamagnetic solids, indicating that the structural form of the cation or its mutual magnetic interactions differs from that in dilute solution. The purpose of this investigation is to establish the structure of the diamagnetic modification of the cation.

## Experimental Section

$[NiL][CF_3SO_3]$, containing the $NiC_{14}H_{18}N_4^+$ cation, was prepared as previously described.[3] Crystals for x-ray studies were obtained by recrystallization of this compound from warm acetonitrile, and were obtained as very dark green hexagonal prisms. (In bulk form these crystals appear black to the eye.) Preliminary precession photographs showed no symmetry other than $\bar{1}$ and no systematic absences; hence the space group is probably $P1$ or $P\bar{1}$. A crystal with distances of 0.182, 0.128, 0.216, and 0.242 mm between faces of the forms {100}, {010}, {110}, and {10$\bar{1}$} was chosen for data collection and was mounted with the [10$\bar{1}$] direction approximately along the spindle axis.

The lattice parameters, obtained as previously described,[7,8] by hand centering of 15 reflections in the range 50° < 2$\theta$ < 72° on a Picker FACS-I diffractometer using Cu K$\alpha_1$ radiation ($\lambda$ 1.540 562 Å), are $a$ = 11.964 (2) Å, $b$ = 12.005 (2) Å, $c$ = 7.308 (1) Å, $\alpha$ = 95.52 (1)°, $\beta$ = 103.26 (1)°, and $\gamma$ = 60.51 (1)° at room temperature, 21 (1) °C. The calculated density, based on one dimer per unit cell, of 1.68 g/cm$^3$ agrees very well with the observed value of 1.68 (2) g/cm$^3$, as measured by flotation in a chloroform-bromoform mixture.

Data were collected in shells of 2$\theta$ by the $\theta$-2$\theta$ scan method using Cu K$\alpha$ radiation prefiltered with Ni foil. The scan range in 2$\theta$ was from 0.9° below the $\alpha_1$ peak to 0.8° above the $\alpha_2$ peak. The takeoff angle was 2.8°. The receiving counter was positioned 32 cm from the crystal preceded by an aperture 3.2 mm high and 2.8 mm wide. The

Table I. Positional and Thermal Parameters for the Atoms of $[Ni(C_{14}H_{18}N_4)]_2(CF_3SO_3)_2$

| ATOM | X[A] | Y | Z | B11[B] | B22 | B33 | B12 | B13 | B23 |
|---|---|---|---|---|---|---|---|---|---|
| NI | -0.074469(66) | 0.030299(66) | 0.15984(10) | 34.7(11) | 29.1(11) | 111.2(24) | -17.31(83) | -15.0(11) | 22.6(11) |
| S | 0.33656(12) | 0.35948(12) | 0.43900(20) | 50.9(15) | 49.9(15) | 167.5(36) | -25.5(11) | -19.1(17) | 23.0(16) |
| F1 | 0.38442(33) | 0.52617(31) | 0.32012(56) | 111.7(45) | 60.1(39) | 269.(11) | -47.3(33) | -0.2(53) | 45.0(49) |
| F2 | 0.54248(29) | 0.32969(34) | 0.33508(50) | 46.6(34) | 103.5(42) | 263.4(92) | -18.2(31) | -2.5(43) | 59.0(47) |
| F3 | 0.37091(37) | 0.38456(36) | 0.10349(52) | 113.2(47) | 103.3(43) | 147.4(92) | -37.5(36) | -5.3(51) | 22.5(47) |
| O1 | 0.38858(39) | 0.38570(40) | 0.63226(56) | 88.4(48) | 92.5(48) | 145.(10) | -54.0(40) | -14.9(54) | 15.7(53) |
| O2 | 0.37853(41) | 0.22486(37) | 0.39131(66) | 102.6(51) | 59.5(43) | 242.(12) | -55.0(38) | -28.1(61) | 12.7(55) |
| O3 | 0.19988(35) | 0.44562(39) | 0.36635(65) | 51.2(40) | 77.2(46) | 257.(13) | -22.3(34) | -20.1(55) | 41.9(58) |
| C15 | 0.41306(51) | 0.40204(48) | 0.29448(78) | 70.5(63) | 44.7(56) | 163.(13) | -20.8(48) | -10.2(69) | 26.9(65) |
| N1 | -0.04447(37) | -0.13824(37) | 0.18503(57) | 34.4(39) | 29.3(40) | 110.5(94) | -17.6(33) | -16.6(48) | 15.4(48) |
| N2 | -0.24800(38) | 0.09106(39) | 0.01958(58) | 40.3(43) | 43.8(46) | 87.9(95) | -27.1(36) | -8.8(51) | 15.4(51) |
| N3 | -0.11107(36) | 0.20278(36) | 0.15943(57) | 39.4(42) | 28.9(40) | 115.0(95) | -18.6(34) | -6.1(51) | 20.7(49) |
| N4 | 0.09298(36) | -0.02569(38) | 0.32157(53) | 39.2(42) | 46.7(49) | 97.(10) | -25.2(39) | -4.2(52) | 14.1(53) |
| C1 | -0.09064(54) | -0.32209(54) | 0.15136(88) | 61.2(60) | 45.4(56) | 214.(15) | -32.1(49) | -10.8(75) | 35.3(73) |
| C2 | -0.12544(51) | -0.18715(48) | 0.11045(80) | 60.8(60) | 39.1(52) | 125.(14) | -30.6(47) | 17.7(73) | -1.6(67) |
| C3 | -0.25025(48) | -0.10960(46) | -0.00499(76) | 50.5(53) | 40.5(49) | 143.(13) | -30.1(42) | -2.5(66) | 10.8(62) |
| C4 | -0.31461(45) | 0.02381(50) | -0.04312(67) | 44.7(48) | 43.3(58) | 103.(11) | -23.1(44) | -1.1(58) | 19.5(61) |
| C5 | -0.45569(51) | 0.08649(52) | -0.14078(83) | 56.3(57) | 53.6(57) | 191.(14) | -37.6(47) | 4.9(72) | 26.7(70) |
| C6 | -0.30857(46) | 0.21979(42) | -0.02047(77) | 42.3(52) | 22.1(45) | 183.(14) | -8.0(40) | 13.2(67) | 18.0(60) |
| C7 | -0.23596(47) | 0.28072(48) | 0.05355(75) | 43.4(52) | 29.1(53) | 177.(13) | -13.5(44) | 1.9(64) | 31.5(64) |
| C8 | -0.07785(53) | 0.39408(53) | 0.22829(86) | 65.4(60) | 55.1(58) | 195.(15) | -40.0(50) | 7.4(74) | 2.8(73) |
| C9 | -0.03093(50) | 0.25345(49) | 0.24312(72) | 60.9(56) | 46.8(54) | 107.(12) | -32.8(46) | 12.6(66) | 3.2(63) |
| C10 | 0.09492(47) | 0.17601(46) | 0.34744(68) | 54.2(55) | 51.3(51) | 100.(11) | -39.5(44) | 3.4(63) | -2.4(60) |
| C11 | 0.15594(47) | 0.04376(50) | 0.38907(72) | 50.1(53) | 49.3(56) | 86.(11) | -32.1(46) | 0.4(62) | -0.9(62) |
| C12 | 0.29114(49) | -0.01759(54) | 0.51149(79) | 49.0(53) | 76.1(60) | 111.(13) | -38.7(47) | -16.3(66) | 11.9(69) |
| C13 | 0.15169(48) | -0.15267(44) | 0.37203(70) | 47.7(54) | 34.9(49) | 112.(12) | -12.7(42) | -2.4(63) | 18.6(57) |
| C14 | 0.07789(43) | -0.21544(46) | 0.29878(69) | 37.3(48) | 28.9(50) | 100.(11) | -13.4(41) | -25.7(57) | 33.3(59) |

[a] Estimated standard deviations in the least significant figure(s) are given in parentheses in this and all subsequent tables. [b] The form of the anisotropic thermal ellipsoid is: $\exp[-(B_{11}h^2 + B_{22}k^2 + B_{33}l^2 + 2B_{12}hk + 2B_{13}hl + 2B_{23}kl)]$. The quantities given in the table are the thermal coefficients $\times 10^4$.

pulse height analyzer was set to admit about 90% of the Cu K$\alpha$ peak. Background counts of 10 s were taken at each end of the scan range. A scan rate of 2° in $2\theta$ per minute was used. Data were collected in the range $5 < 2\theta \leq 125°$.

During the course of data collection eight standard reflections from diverse regions of reciprocal space were measured every 100 reflections. Excessive variations in some of the standards were observed, with variations being between 2 and 20 times those expected on the basis of counting statistics. Data collection was interrupted while different goniometer heads and different crystals were employed to check stability under stationary crystal/stationary counter conditions. Large fluctuations were still observed; these fluctuations disappeared when a basic beryllium acetate crystal was substituted for the crystal of interest. The fluctuations must be crystal-dependent. While the pattern does not appear to be that expected on the basis of anisotropic extinction effects and radiation damage, it may result from extreme sensitivity of the crystal structure to small temperature gradients. Since we could find no immediate solution to the problem of instability and since five of the eight standards were reasonably stable, data collection was continued.

The data were processed as previously described[7,8] using a value of 0.05 for $p$. Of the 3081 reflections measured 2829 are unique, and of these 2374 have $I \geq 3\sigma(I)$ and were used in subsequent refinements. The data were corrected for absorption effects, using a linear absorption coefficient of 31.15 $cm^{-1}$. The transmission factors range from 0.525 to 0.711.

The positions of the nickel atom and all non-hydrogen atoms of the macrocyclic ligand were located on an origin-removed, sharpened Patterson function. The positions of the atoms in the anion were found in a subsequent Fourier map. Ultimately the positions of the hydrogen atoms were found in a difference Fourier map. This supports the assumption made in these calculations that the correct space group is $C_i^1$-$P\bar{1}$. Least-squares refinement, including fixed contributions for the hydrogen atoms (C-H = 0.95 Å and $B_H = B_C + 1$ Å$^2$), an anisotropic model for the Ni atom and the atoms of the anion but an isotropic model for the others, converged to values of $R$ and $R_w$ of 0.115 and 0.162, respectively. In these calculations the usual atomic scattering factors, anomalous terms, procedures, and computer programs were employed.[9]

An analysis of $\sum w(|F_o| - |F_c|)^2$ as a function of setting angles, $|F_o|$, and Miller indices indicated no particular trends; rather the data set was a poor one overall. Consequently refinement was terminated and a low-temperature data set was collected.

A suitable crystal was mounted with G.E. Glyptal to a copper fiber in an Air Products Cryo-tip goniometer equipped with a closed Joule-Thomson cooling cycle. Preliminary surveys indicated that the earlier fluctuations in intensities disappeared when the crystal was held at a constant, low temperature. The temperature chosen for data collection was −117 (3)°. The data were re-collected as previously described for the room-temperature experiment. Data collection was abruptly terminated at $2\theta = 110°$ when a building-wide power failure resulted in the rapid heating-up and then rapid cooling down of the crystal with concomitant shattering of the crystal. The cell parameters at −117 °C are: $a = 12.069$ (2), $b = 11.889$ (2), $c = 7.157$ (1) Å, $\alpha = 98.28$ (1), $\beta = 105.25$ (1), $\gamma = 60.04$ (1)°. Of the 2410 reflections measured, 2194 are unique, and of those 1978 have $I \geq 3\sigma(I)$ and were used in subsequent refinement. One cycle of isotropic least-squares refinement, starting with the parameters of the non-hydrogen atoms derived from the room-temperature data, led to values of $R$ and $R_w$ of 0.183 and 0.278. At this point the data were corrected for absorption; the transmission factors range from 0.547 to 0.739. Two cycles of fully anisotropic, full-matrix least-squares refinement reduced $R$ and $R_w$ to 0.073 and 0.122. A difference Fourier map clearly revealed all the positions of hydrogen atoms. The positions were idealized and used in fixed structure factor contribution in subsequent calculations. The final least-squares refinement of 244 variables and 1978 data converged to values of $R$ and $R_w$ of 0.049 and 0.084. The error in an observation of unit weight is 3.08 electrons. The final difference Fourier map is uninteresting; there are a few peaks of height 0.6 (1) e/Å$^3$ near the Ni atom; other peaks have heights less than 0.3 (1) e/Å$^3$. Final positional and thermal parameters for the non-hydrogen atoms are given in Table I. The calculated hydrogen atom parameters are given in Table II.[10] Root-mean-square amplitudes of vibration are given in Table III.[10] In Table IV[10] we give values of $10|F_o|$ vs. $10|F_c|$ for the reflections used in the refinement.

## Description of the Structure

The crystal structure consists of well-separated dimeric macrocyclic cations and trifluoromethanesulfonate anions. A

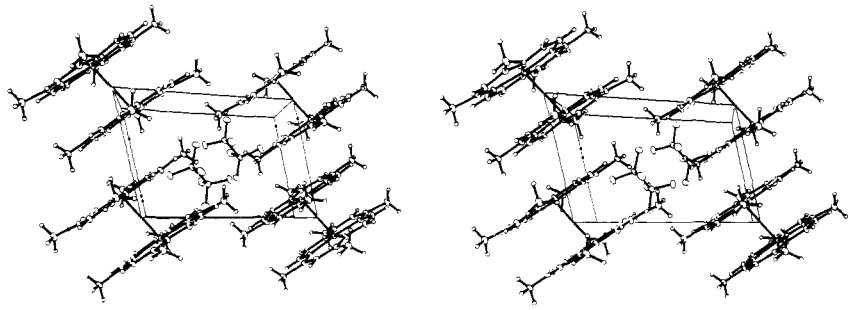

**Figure 1.** A stereoscopic view of the unit cell contents of $[Ni(C_{14}H_{18}N_4)]_2[CF_3SO_3]_2$ illustrating the stacked nature of the dimers. The $x$ axis is horizontal to the right; the $z$ axis is almost vertical, and the $y$ axis is about perpendicular to the paper going away from the reader. Vibrational ellipsoids are drawn at the 20% level. Hydrogen atoms are included and the isotropic thermal parameters are arbitrarily set to 1 Å$^2$.

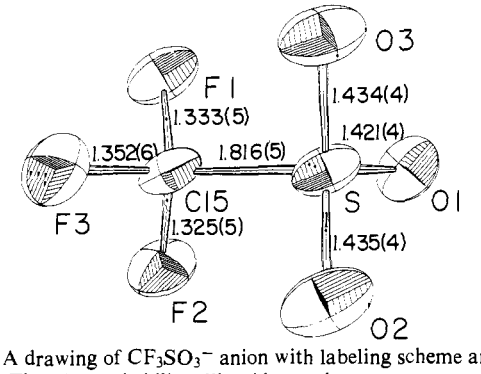


**Figure 2.** A drawing of $CF_3SO_3^-$ anion with labeling scheme and bond distances. The 50% probability ellipsoids are shown.

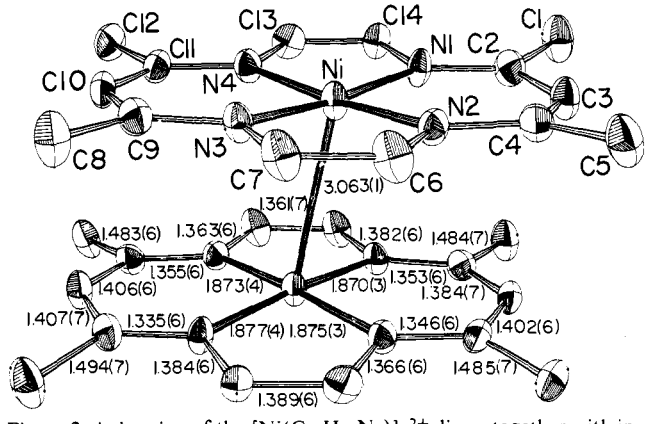


**Figure 3.** A drawing of the $[Ni(C_{14}H_{18}N_4)]_2^{2+}$ dimer together with interatomic distances. The 50% probability ellipsoids are shown.

stereoview of the unit cell is shown in Figure 1. The cationic dimers are stacked along the $z$ direction forming Ni chains with Ni-Ni separations of 3.063 (1) and 4.750 (2) Å and a Ni-Ni-Ni angle of 131.47 (4)°. The least-squares plane defined by the four nitrogen atoms is very close to the $40\bar{4}$ crystallographic plane. The interplanar separation within the dimer is 3.195 Å, whereas it is 3.475 Å between dimers. The anions fit into holes produced by the stacking of the dimers.

Illustrated in Figure 2 are the labeling scheme and principal bond distances for the $CF_3SO_3^-$ anion. Bond angles are found in Table V. Although the geometry of the anion derived from the room-temperature data was far from satisfactory, as judged by the agreement among presumably equivalent bond distances, the results of the low-temperature study (Figure 2) lead to excellent agreement among chemically equivalent parameters.

The overall conformation of $CF_3SO_3^-$ resembles that of staggered ethane. Repulsions between oxygen atoms are apparently greater than those between oxygen atoms and the trifluoromethyl group. As a result the O-S-O and F-C-S angles are greater than 109.5° and the C-S-O and F-C-F angles are less than 109.5° (Table V). All the bond distances in $CF_3SO_3^-$ are identical with those in related structures. The average C-F distance in this structure, 1.34 (1) Å, is very close to that, 1.33 Å,[11,12] found in other trifluoromethyl groups. The average S-O distance of this anion, 1.430 (8) Å, is close to those in other organosulfonate structures, 1.43 Å.[11-13] The S-C distance of $CF_3SO_3^-$, 1.816 (5) Å, is identical with the S-C single bond distance, 1.81 Å.[11,13]

Table V. Bond Angles (deg)

| | | | |
|---|---|---|---|
| $[Ni(C_{14}H_{18}N_4)]_2^{2+}$ | | | |
| Ni'[a]-Ni-Ni''[b] | 131.47 (4) | N(2)-C(4)-C(3) | 119.1 (4) |
| Ni'-Ni-N(1) | 97.56 (14) | N(2)-C(4)-C(5) | 122.7 (4) |
| Ni'-Ni-N(2) | 102.47 (15) | C(3)-C(4)-C(5) | 118.1 (4) |
| Ni'-Ni-N(3) | 88.54 (15) | C(7)-C(6)-N(2) | 115.6 (4) |
| Ni'-Ni-N(4) | 82.90 (14) | C(6)-C(7)-N(3) | 115.1 (4) |
| N(1)-Ni-N(2) | 94.46 (16) | N(3)-C(9)-C(10) | 120.8 (4) |
| N(1)-Ni-N(3) | 173.79 (15) | N(3)-C(9)-C(8) | 120.4 (4) |
| N(1)-Ni-N(4) | 85.50 (16) | C(10)-C(9)-C(8) | 118.8 (4) |
| N(2)-Ni-N(3) | 85.36 (16) | C(9)-C(10)-C(11) | 128.2 (4) |
| N(2)-Ni-N(4) | 174.57 (15) | N(4)-C(11)-C(12) | 120.7 (4) |
| N(3)-Ni-N(4) | 94.09 (15) | N(4)-C(11)-C(10) | 120.8 (4) |
| C(2)-N(1)-C(14) | 119.5 (4) | C(10)-C(11)-C(12) | 118.4 (4) |
| C(2)-N(1)-Ni | 128.1 (3) | N(4)-C(13)-C(14) | 115.6 (4) |
| C(14)-N(1)-Ni | 112.3 (3) | N(1)-C(14)-C(13) | 114.2 (4) |
| C(4)-N(2)-C(6) | 119.6 (4) | $CF_3SO_3^-$ | |
| C(4)-N(2)-Ni | 128.4 (3) | C(15)-S-O(1) | 103.7 (2) |
| C(6)-N(2)-Ni | 112.1 (3) | C(15)-S-O(2) | 103.1 (2) |
| C(9)-N(3)-C(7) | 120.3 (4) | C(15)-S-O(3) | 102.1 (2) |
| C(9)-N(3)-Ni | 128.0 (3) | O(1)-S-O(2) | 115.3 (2) |
| C(7)-N(3)-Ni | 111.7 (3) | O(1)-S-O(3) | 115.2 (2) |
| C(11)-N(4)-C(13) | 119.8 (4) | O(2)-S-O(3) | 115.0 (2) |
| C(11)-N(4)-Ni | 127.8 (3) | S-C(15)-F(1) | 111.8 (3) |
| C(13)-N(4)-Ni | 112.4 (3) | S-C(15)-F(2) | 112.2 (3) |
| N(1)-C(2)-C(3) | 120.1 (4) | S-C(15)-F(3) | 110.9 (3) |
| N(1)-C(2)-C(1) | 122.2 (4) | F(1)-C(15)-F(2) | 107.9 (4) |
| C(3)-C(2)-C(1) | 117.7 (4) | F(1)-C(15)-F(3) | 106.9 (4) |
| C(2)-C(3)-C(4) | 129.4 (4) | F(2)-C(15)-F(3) | 106.8 (4) |

[a] ' is related by center of symmetry $\bar{x}, \bar{y}, \bar{z}$. [b] '' is related by symmetry operation $\bar{x}, \bar{y}, 1 - z$.

There are a number of unusual features associated with the $[NiL]_2^{2+}$ dimer structure (Figure 3). First, the dimer exhibits a Ni···Ni interaction of 3.063 (1) Å. The macrocyclic ligand is essentially planar; the least-squares plane through the 14 inner atoms of the ligand is $6.167x + 0.660y - 6.655z = -1.615$ and the maximum deviation from this plane is −0.036 (5) Å (C(14)). The fact that the Ni atom is displaced 0.112 Å from this plane and 0.095 Å from the least-squares plane through the four nitrogen atoms and that this displacement is toward the other Ni atom of the dimer is a further indication of a Ni···Ni interaction. Values of Ni···Ni distances determined previously in coordination complexes are contained in Table VI. This distance in the present dimer is 0.57 Å longer than in Ni metal[14] and also substantially longer than in most com-

Table VI. Summary of Ni–Ni Distances in Coordination Compounds

| Compound | Formal oxidation state of Ni | Distance | Ref |
|---|---|---|---|
| Ni metal | 0 | 2.49 | 14 |
| Ligand-bridged | | | |
| $[Ni_2(napy)_4Br_2](BPh_4)$[a] | 1.5 | 2.42 | 15 |
| $[Ni_2(PhN_3Ph)_4]$[b] | 2 | 2.38 | 16 |
| $[Ni_2(PhCOS)_4(EtOH)]$ | 2 | 2.50 | 17 |
| $[Ni(Ni(NH_2CH_2CH_2S)_2)_2]Cl_2$ | 2 | 2.73 | 19 |
| $[Ni_2(PhCH_2CS_2)_4]$ | 2 | 2.56 | 18 |
| $[Ni(SEt)_2]_6$ | 2 | 2.92 | 20 |
| $[Ni_2(C_{16}H_{16}N_6)_2]$[c] | 2 | 2.81 | 21 |
| Nonbridged | | | |
| $[Ni(C_{10}H_{14}N_8)]_2$[d] | 2 | 2.78 | 22 |
| $[Ni(C_{14}H_{18}N_4)]_2(CF_3SO_3)_2$ | 2 | 3.06 | This work |
| $[Ni(dmg)_2]$[e] | 2 | 3.25 | 23 |
| $[Ni(dpg)_2]I$[f] | 2.33 | 3.27 | 24 |
| $K_4[Ni_2(CN)_6]$ | 1 | 2.32 | 25 |

Ligands: [a] 1,8-naphthyridine; [b] 1,3-diphenyltriazenide; [c] cyclohexane-1,2-dionebis(2-pyridylhydrazone) dianion; [d] octaaza[14]annulene dianion; [e] dimethylglyoximate; [f] diphenylglyoximate.

Table VII. Closest Contacts in Dimer

| | Distances (Å) | | Distances (Å) |
|---|---|---|---|
| Ni–Ni'[a] | 3.063 (1) | C(3)–C(10)' | 3.244 (6) |
| N(1)–N(3)' | 3.262 (5) | C(4)–C(11)' | 3.291 (6) |
| N(2)–N(4)' | 3.236 (5) | C(5)–C(12)' | 3.489 (7) |
| C(1)–C(8)' | 3.571 (8) | C(6)–C(13)' | 3.312 (6) |
| C(2)–C(9)' | 3.322 (6) | C(7)–C(14)' | 3.330 (6) |

[a] ' is related by center of symmetry $\bar{x}, \bar{y}, \bar{z}$.

plexes in which Ni atoms are juxtaposed by ligand bridges.[15-21] This is especially the case for dimers of the $[Cu(OAc)_2]_2$-type structure,[15-17,19] whose structure and properties are indicative of direct Ni···Ni interactions that can sensibly be construed as arising from direct metal–metal bonding. Examples of Ni···Ni distances in nonbridged complexes[22-25] are included in Table VI. Of these the structure of $[NiL]_2^{2+}$ is most profitably compared with that of the dimeric octaaza[14]annulene complex $[Ni(C_{10}H_{14}N_8)]_2$.[22] The two structures are very similar and comparisons are given below. The Ni···Ni interactions in $[Ni(dmg)_2]$ and $[Ni(dpg)_2]I$ are not generally described as metal–metal bonds. Structures and bonding in multinuclear $d^8$ systems have recently been treated by Fackler.[26]

A second unusual feature of the cation is that the macrocyclic ligands of the dimer are eclipsed; this maximizes rather than minimizes nonbonding interactions. The distances of closest contacts in the dimer are listed in Table VII. The interplanar separation between the least-squares planes defined by the four nitrogen atoms, 3.195 Å, is in the repulsive range for nonbonding interactions.[27] Obvious nonbonding repulsion of the four methyl groups is observed, as indicated by separations of 3.49 and 3.59 Å for atoms C(5)–C(12)' and C(1)–C(8)', respectively. Hence an attractive interaction between the two macrocyclic ligands in addition to the Ni–Ni bond must be invoked to account for the eclipsed conformation.

A third feature of the cation is that the double bonds of the macrocyclic ligand are essentially delocalized. The average C–C and C–N distances in the six-membered ring, 1.400 (10) and 1.347 (9) Å, are very close to the accepted C–C distance of benzene and the C–N distance of pyridine. The C–C and C–N distances of the five-membered ring, 1.38 (2) and 1.37 (1) Å, respectively, are also intermediate between those expected for single and double bonds.

The coordination geometry about the Ni atom is square-pyramidal. The Ni atom is displaced by only 0.095 Å from the mean $N_4$ coordination plane. The average Ni'–Ni–N angle is 93 (2)°. The average Ni–N distance, 1.874 (3) Å, lies toward the short end of bond distances of this type. It is, however, somewhat longer than those in most closely realted complexes **5** and **6**, of the octaaza[14]annulene type. These complexes are

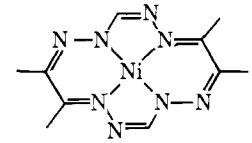

**5**

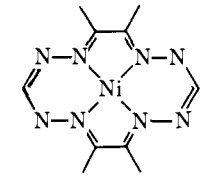

**6** (half dimer)

isomeric with the empirical formula $Ni(C_{10}H_{14}N_8)$; in the crystalline state **5** is monomeric with Ni–N = 1.800 (2) Å[28] and **6** (Table VI) is dimeric with Ni–N = 1.832 (5) Å.[22]

Table VIII. Comparison of the $[Ni(C_{10}H_{14}N_8)]_2$ and $[Ni(C_{14}H_{18}N_4)]_2^{2+}$ Structures

| | $[Ni(C_{10}H_{14}N_8)]_2$ | $[Ni(C_{14}H_{18}N_4)]_2^{2+}$ |
|---|---|---|
| Ni–Ni metal distance | 2.788 (2) Å | 3.063 (1) Å |
| Ni–Ni distance between two adjacent dimers | 3.800 (3) Å | 4.750 (2) Å |
| Ni–Ni–Ni angle | 169.48 (5)° | 131.47 (4)° |
| Interplanar[a] separations within | | |
| dimer and | 3.00 Å | 3.19 Å |
| between dimers | 3.59 Å | 3.47 Å |
| Ni atom out of plane[a] distance | 0.104 Å | 0.095 Å |
| Conformation of macrocyclic ligands in dimer | Eclipsed | Eclipsed |
| Double bonds arrangement | Delocalized | Delocalized |
| Idealized dimer symmetry | $D_{2h}$ | $D_{2h}$ |
| Macrocyclic ligand's charge | 2– | 1– |
| No. of $\pi$ electrons | 16 | 15 |
| Bonds[b] between ligand–ligand | 2 weak $\pi$ bonds | 1 weak $\pi$ bond |
| Ni–Ni | $\sigma$ and $\delta$ bonds | $\sigma$ and $\delta$ bonds |
| Species in solid | Dimer | Dimer |
| Species in solution | Dimer | Dimer $\rightleftharpoons$ monomer |

[a] The plane is defined by the four coordinated nitrogen atoms. [b] According to the bonding scheme proposed by Peng and Goedken.[22]

## Discussion

The most closely related structure to $[NiL]_2^{2+}$ presently known is that of $[Ni(C_{10}H_{14}N_8)]_2$ (**6**). Some important features of the two complexes are compared in Table VIII. To account for the Ni···Ni interaction and the eclipsed ligand arrangement in the octaaza[14]annulene dimer, Peng and Goedken[22] have proposed a qualitative bonding model which has led to the correct prediction of the same two structural features in $[NiL]_2^{2+}$. This model, together with other relevant symmetry-based orbital interactions for $d^8$–$d^8$ dimers,[26] has been described adequately elsewhere.[22] Here it is proposed that the stereochemically determinant bonding interactions in the $D_{2h}$ dimer involve mixing of the local metal orbitals $d_{z^2}$ and $d_{xy}$, affording doubly occupied Ni···Ni $\sigma$ and $\delta$ orbitals, with antibonding components $\sigma^*$ and $\delta^*$ unoccupied. Superimposed upon these interactions is direct ligand–ligand $\pi$-bonding involving the $b_{1u}$ orbital of each half dimer, whose symmetry has been previously deduced from an analysis of $\pi$-spin densities of $[NiL]^+$, as determined from solution EPR studies.[3] The symmetric linear combination ($a_{1g}$) is occupied, resulting in the spin-pairing necessitated by the diamagnetism of $[NiL]_2^{2+}$, and the antibonding combination ($b_{1u}$*) is unoccupied. The totality of the bonding interactions involves metal–metal $\sigma$ and

$\delta$ bonding and ligand–ligand $\pi$-bonding, and is doubtless relatively weak, as judged by the tendency of $[NiL]_2^{2+}$ to dissociate in solution. In formulating this simple bonding scheme each half-dimer has been treated as $[Ni^{II}L\cdot^{-}(15\pi)]^{+}$.[3] The alternative possibility, $[Ni^{III}L^{2-}(16\pi)]^{+}$ $[Ni^{I}L^{0}(14\pi)]^{+}$, is inconsistent with the equivalence of each half-dimer. This arrangement would result in one antiaromatic $16\pi$ ligand with fixed double bonds (as observed for **5**[28]) and an aromatic $14\pi$ delocalized ligand, contrary to observation.

**Acknowledgments.** This research was supported by National Science Foundation Grants GP-40089X (MIT) and GP-38034X (Northwestern). We thank Dr. M. Cowie for assistance with the data collection at low temperature.

**Supplementary Material Available:** The calculated hydrogen atom parameters (Table II), root-mean-square amplitudes of vibration (Table III), and the list of structure amplitudes (Table IV) (16 pages). Ordering information is given on any current masthead page.

## References and Notes

(1) (a) Northwestern University; (b) Department of Chemistry, Stanford University, Stanford, California 94305.
(2) T. J. Truex and R. H. Holm, *J. Am. Chem. Soc.*, **94**, 4529 (1972).
(3) M. Millar and R. H. Holm, *J. Am. Chem. Soc.*, **97**, 6052 (1975); *J. Chem. Soc., Chem. Commun.*, 169 (1975).
(4) S. C. Tang, S. Koch, G. N. Weinstein, R. W. Lane, and R. H. Holm, *Inorg. Chem.*, **12**, 2589 (1973).
(5) S. C. Tang and R. H. Holm, *J. Am. Chem. Soc.*, **97**, 3359 (1975). This paper contains a brief review of other types of metal complex oxidative dehydrogenation reactions.
(6) T. J. Truex, Ph.D. Thesis, M.I.T., 1972; M. Millar and R. H. Holm, unpublished observations.
(7) P. W. R. Corfield, R. J. Doedens, and J. A. Ibers, *Inorg. Chem.*, **6**, 197 (1967).
(8) R. J. Doedens and J. A. Ibers, *Inorg. Chem.*, **6**, 204 (1967).
(9) B. A. Averill, T. Herskovitz, R. H. Holm, and J. A. Ibers, *J. Am. Chem. Soc.*, **95**, 3523 (1973).
(10) See paragraph at end of paper regarding supplementary material.
(11) "International Tables for X-Ray Crystallography", Vol. III, Kynoch Press, Birmingham, England, 1968, p 225.
(12) J. B. Spencer and J. Lundgren, *Acta Crystallogr., Sect. B*, **29**, 1923 (1973).
(13) S. K. Arora and M. Sundaralingam, *Acta Crystallogr., Sect. B*, **27**, 1293 (1971).
(14) "Handbook of Chemistry and Physics", 54th ed, Chemical Rubber Publishing Co., Cleveland, Ohio, 1973–1974, p F-127.
(15) L. Sacconi, C. Mealli, and D. Gatteschi, *Inorg. Chem.*, **13**, 1985 (1974).
(16) M. Corbett and B. Hoskins, *Chem. Commun.*, 1602 (1969).
(17) M. Bonamico, G. Dessy, and V. Fares, *Chem. Commun.*, 697 (1969); G. A. Melson, P. T. Greene, and R. F. Bryan, *Inorg. Chem.*, **9**, 1116 (1970).
(18) M. Bonamico, G. Dessy, and V. Fares, *Chem. Commun.*, 1106 (1969).
(19) C. H. Wei and L. F. Dahl, *Inorg. Chem.*, **9**, 1878 (1970).
(20) P. Woodward, L. F. Dahl, E. W. Abel, and B. C. Cross, *J. Am. Chem. Soc.*, **87**, 5251 (1965).
(21) N. Bailey, T. James, J. McCleverty, E. McKenzie, R. Moore, and J. Worthington, *J. Chem. Soc., Chem. Commun.*, 681 (1972).
(22) S.-M. Peng and V. L. Goedken, *J. Am. Chem. Soc*, in press.
(23) D. Williams, G. Wohlauer, and R. Rundle, *J. Am. Chem. Soc.*, **81**, 755 (1959).
(24) A. Gleizes, T. J. Marks, and J. A. Ibers, *J. Am. Chem. Soc.*, **97**, 3545 (1975).
(25) O. Jarcow, H. Schultz, and R. Nast, *Angew. Chem.*, **82**, 43 (1970).
(26) J. P. Fackler, Jr., *Prog. Inorg. Chem.*, **21**, 55 (1976).
(27) J. Williams, P. Stang, and P. Schleyer, *Annu. Rev. Phys. Chem.*, **95**, 5773 (1973).
(28) V. L. Goedken and S.-M. Peng, *J. Am. Chem. Soc.*, **95**, 5773 (1973).

# The Stabilization of $\alpha$- and $\beta$-Diimines: Hexaammineruthenium(III), -osmium(III), and -platinum(IV) Condensed with $\alpha$- and $\beta$-Diketones

**I. P. Evans, G. W. Everett, and A. M. Sargeson***

*Contribution from the Research School of Chemistry, The Australian National University, Canberra. A.C.T., Australia.* *Received April 27, 1976*

**Abstract:** Biacetyl condenses with $Ru(NH_3)_6^{3+}$ in basic solution to yield the chelated diimine complex $[(NH_3)_4 Ru(NH{=}C(CH_3)(CH_3)C{=}NH)]^{2+}$ which oxidizes readily with $Br_2$ (aq) to give the Ru(III) ion, $E = 0.56$ V. The condensation requires coordinated amide ions to capture the carbonyl groups followed by elimination of water. In basic solution the Ru(III) ion reduces to the Ru(II) ion in a reaction which apparently involves some intramolecular reduction by the ligand. Analogously $Os(NH_3)_6^{3+}$ captures biacetyl to give the trans bis-diimine complex with approximately the same redox potential. Acetylacetone and trifluoroacetylacetone also condense with $Pt(NH_3)_6^{4+}$ to stabilize a chelated diimine anion.

Several intramolecular reactions between carbonyl centers and coordinated amide ions leading to carbinolamine and imine chelates have been observed recently.[1-5] Although analogous chelated imines have been known for many years with labile metal ions, the route whereby the chelate formed has not been ascertained. Condensation of the imine could occur off or on the metal complex with such labile systems.

The present paper investigates the prospect of forming chelates using coordinated nucleophiles and reactive dicarbonyl systems in intermolecular reactions.[6] The investigation is part of a general program to develop rational syntheses of chelate complexes and organic molecules where the metal center activates, protects, and organizes the syntheses.

## Experimental Section

$^1$H NMR spectra were obtained with a JEOL 100-MHz Minimar spectrometer at 30 °C using tetramethylsilane ($Me_4Si$) as the internal reference. INDOR nitrogen spectra were obtained using a Varian HA-100 spectrometer. Electrochemical measurements were performed using a PAR Model 170 electrochemistry system in water/0.1 M $NaClO_4$ vs. a saturated calomel electrode. A three-electrode iR compensated system with a platinum auxiliary electrode was used throughout. Both the ac polarography and cyclic voltammetry were performed at a Beckmann platinum disk stationary electrode with an area of ~0.27 $cm^2$ at a scan rate of 200 mV $s^{-1}$. Phase sensitive ac measurements were made at 80 Hz with a phase angle of 90° with respect to the charging current and with an ac perturbation of 5 mV peak-peak. Solutions were degassed with nitrogen before measurements were taken at 22 °C under a blanket of inert gas.

Spectrophotometric measurements were made with either a Cary 14 or a 118C spectrophotometer. Determinations of pH were made with a Radiometer Model pH meter using a $TTA_3$ electrode assembly.

**Kinetics (25 °C).** (a) The formation of I from $Ru(NH_3)_6Cl_3$ was followed spectrophotometrically at 465 nm ($\lambda_{max}$ for I) at constant pH using 0.05 M collidine buffer (pH 7.36, $\mu$ = 1.0 M NaCl). The